Wind and Structures, *Vol. 18, No. 5 (2014) 511-528*
DOI: http://dx.doi.org/10.12989/was.2014.18.5.511

Wake galloping phenomena between two parallel/unparallel cylinders

Sunjoong Kim and Ho-Kyung Kim*

Department of Civil and Environmental Engineering, Seoul National University, Gwanak-ro, Gwanak-gu, Seoul 151-744, South Korea

(Received August 23, 2013, Revised January 11, 2014, Accepted January 18, 2014)

Abstract. The characteristics of wake galloping phenomenon for two parallel/unparallel circular cylinders were investigated via wind tunnel tests. The two cylinders were initially deployed in parallel and wake galloping phenomena were observed by varying the center-to-center distance. The effect of an unparallel arrangement of two cylinders was next investigated by fixing the spacing ratio of one side of the cylinders at 5.0*D* and the other side at 3.0*D*, in which *D* represents the diameter of the cylinder. For the unparallel disposition, the 5.0*D* side showed a small, limited vibration while the 3.0*D* side produced much larger amplitude of vibration, resulting in a rolling motion. However, the overall amplitude appeared to decrease in unparallel disposition when compared with the amplitude of the 3.0*D* - 3.0*D* parallel case. This represents the mitigation effect of wake galloping due to the unparallel disposition between two cylinders. Flow visualization tests with particle image velocimetry were conducted to identify flow fields between two cylinders. The test results demonstrate the existence of a complex interaction of the downstream cylinder with the shear layer generated by the upstream cylinder. When the spacing ratio was large enough, the shear layer was not observed and the downstream cylinder showed only limited random vibration.

Keywords: flow visualization; particle image velocimetry (PIV); shear layer; stay cable; unparallel; wake galloping; wind tunnel test

1. Introduction

Wake galloping occurs when closely spaced circular cylinders are exposed to a high wind velocity, resulting in large amplitude oscillations in downstream cylinders. This phenomenon has been observed in stay cables of cable-stayed bridges in Japan (Land Development Technology Research Foundation 1989) and represents a risk of causing a fatigue problem on strands at the end clamps.

Several guidelines (PTI 2001, SETRA 2002, Caetano 2007) proposed formulas for use in predicting the onset wind velocity of wake galloping in terms of spacing ratio, natural frequency, diameter, mass and the damping ratio of a cable. Among these parameters, the spacing ratio (L/D) is one of the governing parameter for the occurrence of wake galloping, where L is the center-to-center distance of two cylinders and D is the diameter of the cylinder. Field observations in Japan (Land Development Technology Research Foundation 1989) reported that wake galloping

*Corresponding author, Professor, E-mail: hokyungk@snu.ac.kr

http://www.techno-press.org/?journal=was&subpage=8 ISSN: 1226-6116 (Print), 1598-6225 (Online)

was observed when the spacing ratio was in the range between 4 and 5. Kumarasena *et al*. (2007) also reported that the onset velocity of wake galloping increased by 3.2 times when the spacing ratio increased from 2~6 to 10. The KSCE guideline (2006) specifies the potential conditions for wake galloping to be a spacing ratio of 3~6 times to that for the diameter.

Numerical and experimental analyses have been carried out to identify the vibrational characteristics in a single and/or tandem cable. A numerical analysis of wake galloping using quasi-steady theory found that a critical reduced wind velocity of wake galloping depends on the Scruton number, turbulence intensity and arrangements of the cylinder (Błazik-Borowa and Flaga 1998). In experimental studies, attempts were also made to investigate the dynamic behavior and the vibration mechanism of a single circular cylinder through wind tunnel testing (Cheng *et al.* 2003, Cheng and Tanaka 2005). Especially, Kim and Sakamoto (2006) performed forced-vibration tests and found that the fluctuating lift forces during vortex excitation were significantly larger than those of a stationary situation. Tokoro *et al*. (2000) carried out full-scale wind tunnel tests, in which the downstream cylinder was subjected to wake galloping tuned to the first vertical mode for the case of L/D = 4.3 and a larger amplitude was observed with an increase in wind velocity.

The mitigation measures were also investigated via wind tunnel experiments. A series of wind tunnel tests (Kim *et al*. 2011) verified that an increase in structural damping was not effective in reducing the amplitude of the vibration of wake galloping. Li *et al.* (2013) evaluated the effect of vibration suppression by the connecting point of twin cables through full-scale wind tunnel tests with three-dimensional aeroelastic cable models.

However, aforementioned studies dealing with wake galloping problems only considered the case of a parallel disposition between two cables. Recently, a cable-stayed bridge was constructed with a so-called ‘three-way’ cable system in which the two planes of the cables are separated to both sides of the deck at the center span similar to a conventional cable-stayed bridge but are merged together at the center of the deck at the side spans, as shown in Fig. 1 (Kim *et al*. 2012). Fig. 1(b) shows the configuration of two stay cables in which the gap distances vary from the tower to deck. The gap distances at the deck side are smaller than the critical distance for wake galloping according to the design guidelines, while the tower sides show sufficient gaps. The general design rules and the open literatures for parallel disposed cables are no longer applicable to this case.

(a) Overall views

(b) The disposition of stay cables at the side span

Fig. 1 The investigated bridge

This paper presents wake galloping measurements of a pair of cylinders in a tandem arrangement including an unparallel disposition. A series of wind tunnel tests were carried out in order to evaluate the instability conditions for wake galloping and the mitigating effect due to an unparallel disposition. PIV tests were also conducted to estimate the flow-structure-interaction between the two cylinders.

2. Wake galloping in parallel cylinders

Prior to the wind tunnel test for the unparallel cylinders, the behavior of parallel cylinders was first estimated for various gap distances between the two cylinders. Through this fundamental experiment, the reproducibility of wake galloping for parallel cylinders can be confirmed which demonstrates the validity of the test setup used in the remainder of this study.

2.1 Experimental setup

The purpose of the tests was to evaluate the displacement of the cylinder as a function of spacing ratio and wind velocity. A series of tests were carried out in a wind tunnel at the Department of Civil and Environmental Engineering, Seoul National University. The test section of the wind tunnel is 1.0 m in width, 1.5 m in height. The maximum wind velocity is 20 m/s with a turbulence intensity of less than 1.0%.

A two-dimensional cylinder model on a scale of 1:2.5 consisted of steel rods and an acrylic 100 mm-diameter and 900 mm-long rod. The model was mounted on supporting devices, as shown in Fig. 2. Four coil springs, installed at angles of 45˚, allowed the cylinder to move freely with respect to the along-wind and perpendicular directions. The target natural frequencies of the cylinder were adjusted with spring constants. The displacement of the cylinder was monitored by vision-based displacement transducers and the wind velocity was measured using an X-type hot wire anemometer. For the parallel arrangement, the spacing ratio was changed from a close to a wide spacing (L/D = 3.0, 3.5, 4.0, 4.5, 5.0, 6.0, 7.0 and 8.0). The unequivocal definition of D and L is shown in Fig. 3.

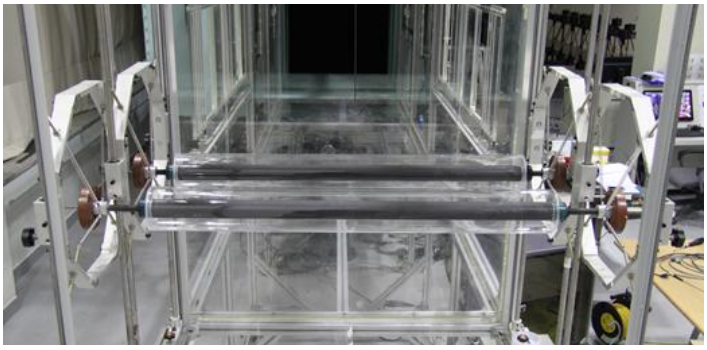

Fig. 2 Parallel cylinders in a wind tunnel

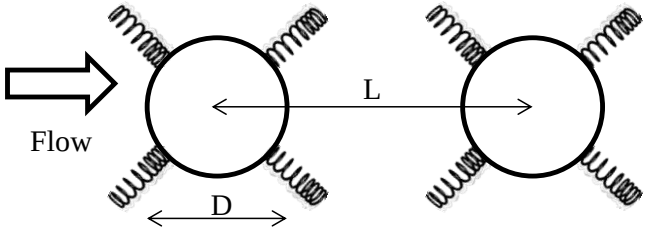

Fig. 3 Diameter (D) and spacing (L) between two cylinders

2.2 Similitude laws

The section models for both cylinders were prepared with a length scale of $\lambda_L = L_m/L_p = 1/2.5$, where L_m and L_p represent the length of the model and prototype, respectively. The frequency scale of $\lambda_f = f_m/f_p = 1/\lambda_T = 3.28$, where λ_T is the time scale and f_m and f_p represent the frequency of the model and prototype, respectively, is adopted. The scaling of reduced wind velocity was satisfied as

$$\left(\frac{U}{fB}\right)_m = \frac{\lambda_L / \lambda_T}{\lambda_f \lambda_L}\left(\frac{U}{fB}\right)_p = \left(\frac{U}{fB}\right)_p \tag{1}$$

where U is the wind velocity and the subscripts m and p denote the model and the prototype, respectively. Table 1 shows the structural parameters of the prototype cables and the test cylinders.

Due to limitations associated with the wind tunnel facility, it was not possible to satisfy the Reynolds number in the wind tunnel setup. Fig. 4 shows the change in drag coefficient of the testing cylinder as a function of Reynolds number. The maximum Reynolds number realized was 2.0×10^5 categorized as a sub-critical range and the observations of wake galloping were performed in this range.

Table 1 Setup parameters of cylinder model

Parameters	Reduced scale	Prototype	Model (target)	Model (measured)
Length (m)	λ_L =1/2.5	2.54	0.900	0.900
Diameter (m)	λ_L	0.250	0.100	0.100
Mass (kg/m)	λ_L^2	92.426	14.788	15.210
1st Frequency (Hz)	λ_f =3.28	0.599	1.965	1.97
Damping ratio (%)	1	0.190	0.190	0.190
Scruton number	1	2.341	2.341	2.408

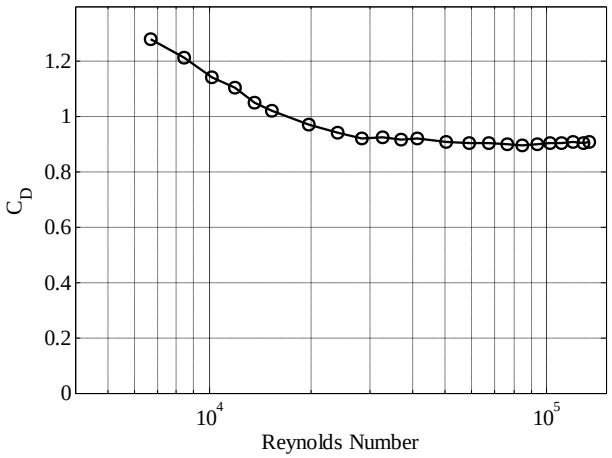

Fig. 4 Change of measured drag coefficient of cylinder according to Reynolds number

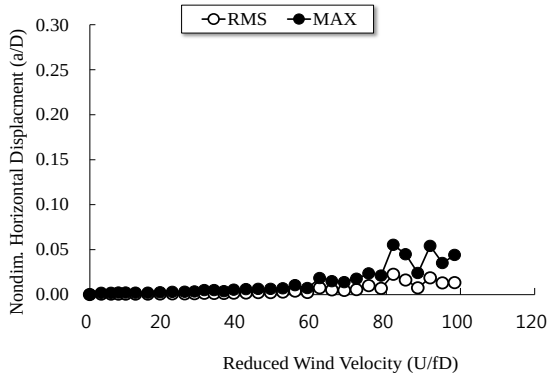

(a) Horizontal response of the upstream cylinder

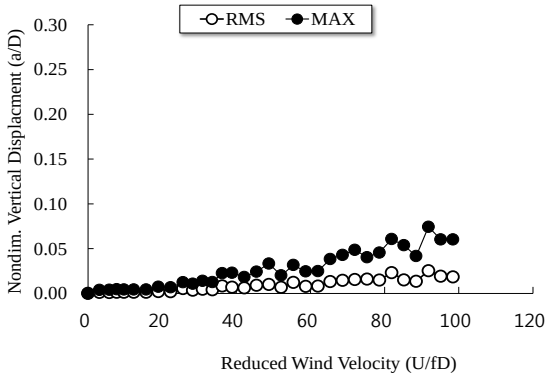

(b) Vertical response of the upstream cylinder

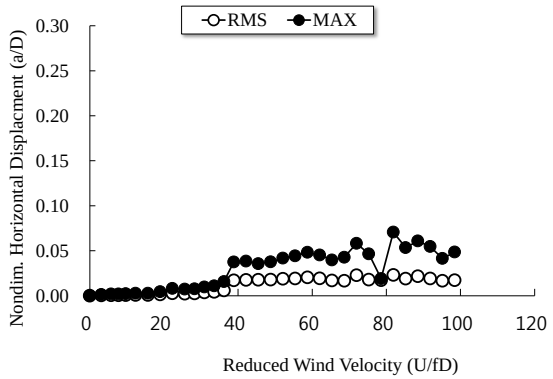

(c) Horizontal response of the downstream cylinder

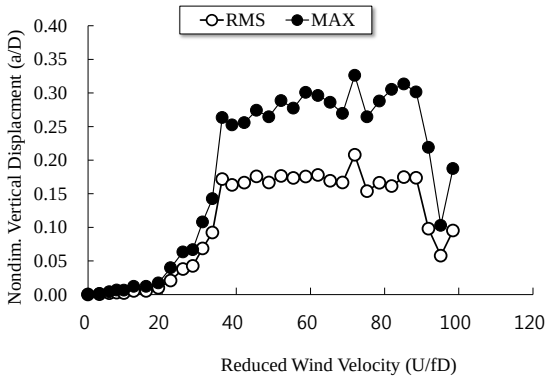

(d) Vertical response of the downstream cylinder

Fig. 5 Non-dimensional displacement of parallel cylinders (*L/D* = 3.0)

2.3 Response of the downstream cylinder in parallel disposition

The normalized displacements of the upstream and downstream cylinders are shown in Fig. 5 for an *L/D* of 3.0. Root Mean Square (RMS) and maximum values of normalized horizontal and vertical displacement of the cylinders were obtained to evaluate the amplitude level of wake galloping and to evaluate the possibility that the allowable limitation could be exceeded. The allowable amplitude of the vibration is defined as *L*/1600 = 0.57 (KSCE, 2006).

As can be seen, severe vibrations in the vertical direction were observed for the downstream cylinder as the wind velocity increased. Wake galloping was observed when the reduced wind velocity (*U/fD*) reached 28.3 and a huge vibration appeared starting at *U/fD* = 36.2. Fig. 6 shows the trajectory of the motion of the downstream cylinder for the case of the maximum vertical response at*U/fD* = 74.7.

The normalized displacements of the upstream and downstream cylinders are shown in Fig. 7 for the case of *L/D*= 3.5. Similar to the case of *L/D* = 3.0, nomeaningful response was observed in the upstream cylinder for this case. Wake galloping was initiated starting at *U/fD* = 33.5 and increased with increasing wind velocity. After the peak response at *U/fD* = 58.7, the amplitude of the vibration gradually decreased with increasing wind velocity.

By increasing the spacing ratio, it was possible to measure the vertical amplitudes of wake galloping and the results are shown in Fig. 8. Fig. 9 also shows the change in amplitude as a function of increasing wind velocity. As expected, by increasing the spacing ratio, the response gradually decreased and the onset wind velocity for wake galloping slightly increased. In fact, the risk of wake galloping was identified only for the cases of *L/D* = 3.0 and 3.5 and the amplitude of the vibration gradually decreased when the spacing ratio exceeded 4.0. All cases satisfied the acceptable amplitude of vibration for the range of wind velocity being considered. The results were in good agreement with the design guidelines which specify that wake galloping becomes a risk factor for spacing ratios in the range of 3.0*D* to 6.0*D*.

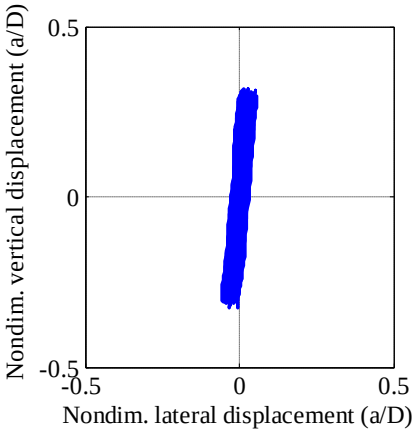

Fig. 6 The trajectory of motion for the downstream cylinder (*L/D* = 3.0, *U/fD* = 74.7)

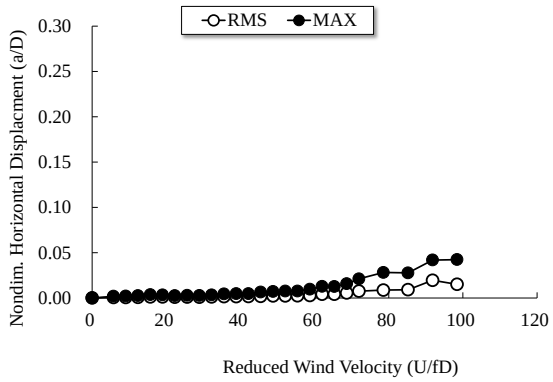

(a) Horizontal response of the upstream cylinder

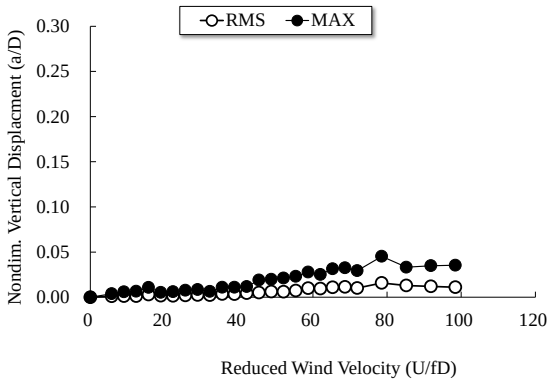

(b) Vertical response of the upstream cylinder

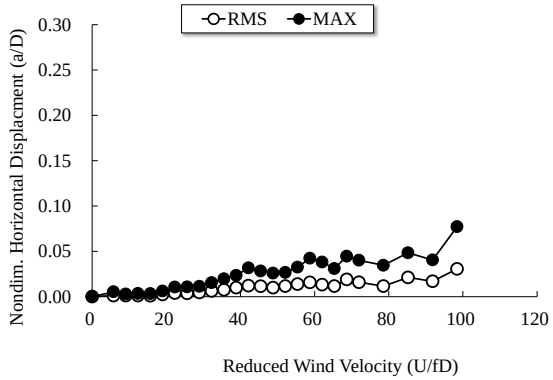

(c) Horizontal response of the downstream cylinder

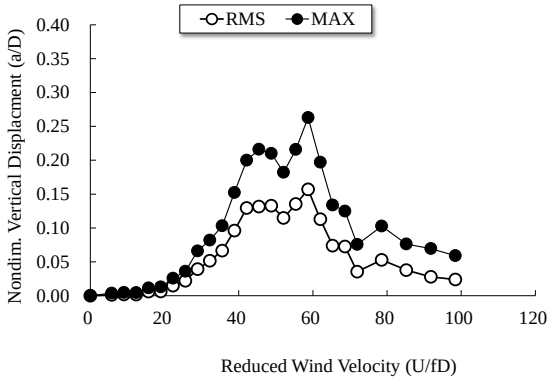

(d) Vertical response of the downstream cylinder

Fig. 7 Non-dimensional displacement of parallel cylinders (L/D = 3.5)

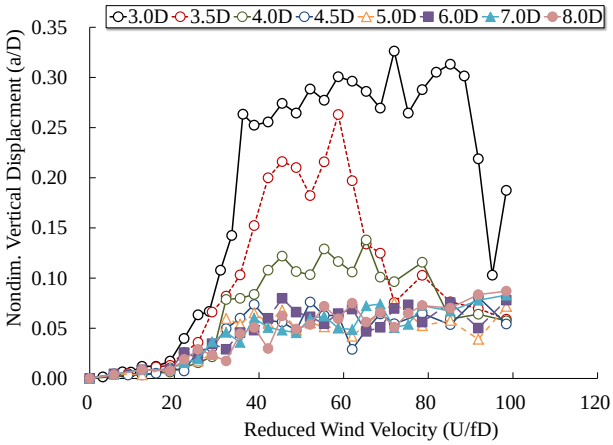

Fig. 8 Non-dimensional vertical displacement of the downstream cylinder as a function of spacing ratio and reduced wind velocity

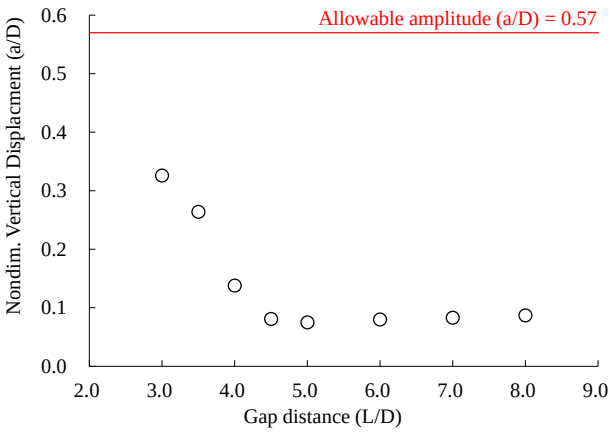

Fig. 9 Maximum non-dimensional vertical displacement of the downstream cylinder as a function of spacing ratio

Fig. 10 shows the time histories for the vertical displacement of the downstream cylinder for the cases of *L/D* = 3.0 and 7.0 at the wind velocity for achieving maximum vertical displacement. As can be seen, a nearly single harmonic motion was observed at *L/D* = 3.0 while a random vibration was observed for the case of *L/D* = 7.0. The peak factor, defined as the ratio between the maximum amplitude to the RMS, was 1.54 for the case of the *L/D* = 3.0 while it approached 2.59 for the case of *L/D* = 7.0. The former is for the value of a harmonic motion while the latter is for a more randomly changed response such as a buffeting response in a turbulent flow.

Fig. 11 shows the results of an FFT analysis of the vertical displacement for the cases of *L/D* = 3.0, 4.0 and 7.0 at the wind velocity for achieving a maximum vertical displacement. For the case of *L/D* = 3.0, the first vertical mode was dominant. For *L/D* = 4.0, for which wake galloping started to decrease, the amplitude of the first mode decreased to 1/3 the level compared to *L/D* = 3.0 and a second mode appeared. For *L/D* = 7.0, the contribution of the first mode was becoming much smaller.

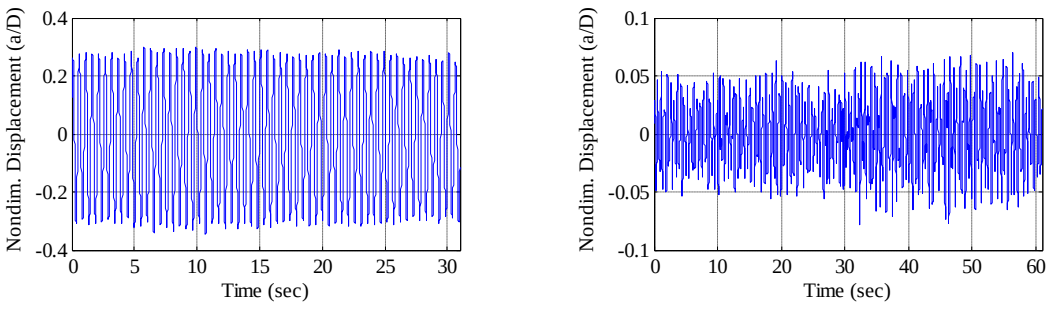

(a) *L/D* = 3.0 (b) *L/D* = 7.0

Fig. 10 Time histories for the non-dimensional vertical displacement of the downstream cylinder

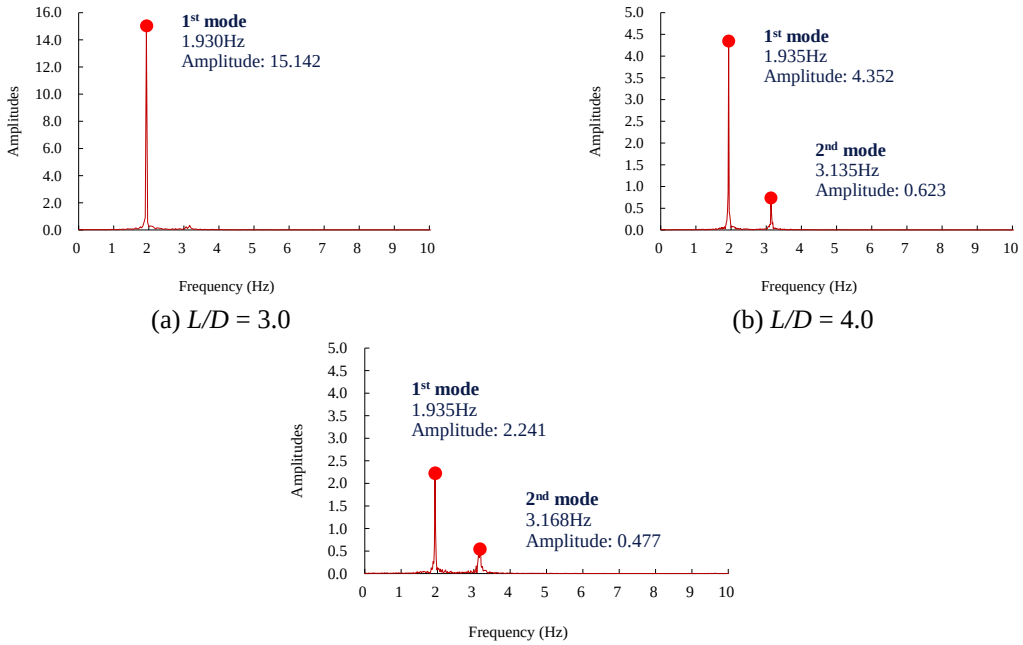

(a) L/D = 3.0 (b) L/D = 4.0

(c) L/D = 7.0

Fig. 11 FFT analysis of the vertical displacement of the downstream cylinder

3. Wake galloping in unparallel cylinders

The effect of the unparallel disposition of two cables was investigated by fixing the spacing ratio of one side of the cables at 3.0D and the other side at 5.0D, as shown in Fig. 12. The portion of the cylinder for a spacing ratio between 3.0D ~ 4.0D represents the 'wake galloping range' based on wind tunnel tests results obtained using parallel cylinders. The other half length of the cylinders is free from wake galloping. Fig. 12 shows the model set-up for unparallel cylinders and the definition of the wake galloping range.

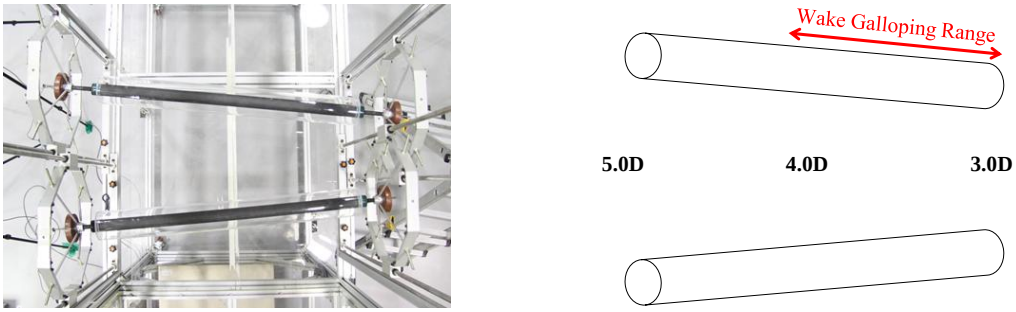

(a) Set-up of unparallel cylinders in a plane view (b) The definition of the wake galloping range

Fig. 12 Unparallel deployment of two cylinders

In Fig. 13, the amplitudes of vibration between the unparallel and parallel cases are compared. For a spacing ratio of 3.0*D* for one side and 5.0*D* for the other side, the amplitude of wake galloping is measured at the 3.0*D* side and the results are shown in Fig. 13. This figure demonstrates that wake galloping in the 3.0*D*-5.0*D* case is mitigated to the level of the 5.0*D* -5.0*D* case which was shown in Fig. 8.

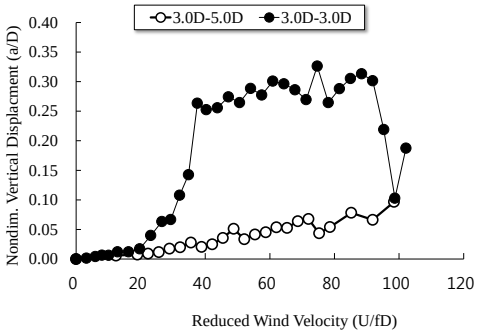

Fig. 13 Maximum non-dimensional displacement of the downstream cylinder at the side of 3.0*D* for unparallel (3.0*D*-5.0*D*) and parallel (3.0*D*-3.0*D*) dispositions

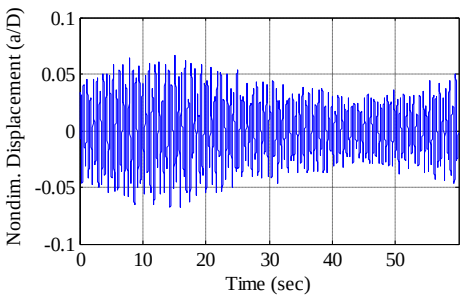

(a) Time histories

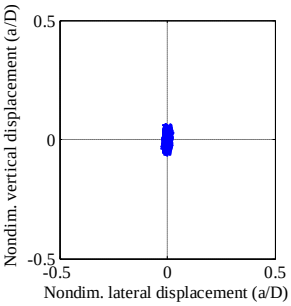

(b) The trajectory of motion

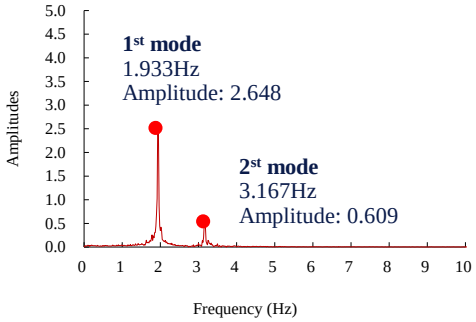

(c) FFT analysis

Fig. 14 Non-dimensional vertical displacement of downstream cylinder at the 3.0*D* side for the unparallel disposition (*L*/*D* = 3.0-5.0)

Fig. 14(a) shows the time histories for the vertical displacement of the downstream cylinder at the 3.0*D* side for the unparallel disposition. While a harmonic motion was observed in the case of a parallel disposition of 3.0*D*-3.0*D* as shown in Fig. 10(a), the unparallel disposition of 3.0*D*-5.0*D* produces an irregular vibration similar to that monitored in the case of a 7.0*D*-7.0*D* parallel disposition. The trajectory of the downstream cylinder in Fig. 14(b) is also comparable to the results for the parallel case in Fig. 6. The result of an FFT analysis of the unparallel case is shown in Fig. 14(c). Contrary to the case of parallel disposition, in which only the first vertical mode was observed, as shown in Fig. 11(a), the unparallel disposition excites the second mode which results in the development of a rolling motion. Consequently, the unparallel disposition of the two cylinders clearly mitigates wake galloping phenomena compared to the parallel disposition.

4. Flow visualization between two cylinders

A series of vibration tests showed that the large spacing ratio contributes to a decrease in wake galloping. Since the mitigation of vibration is closely related to changes in the flow stream, particle image velocimetry (PIV) measurements are carried out, in an attempt to estimate the flow field around cylinders that are in a tandem arrangement. PIV has been widely used to evaluate the flow field around the cylinder (Lee and Lee 2008, Ozgoren *et al.* 2011). Relevant researches of Kim *et al*. (2009) and Assi *et al*. (2010) reported flow interactions between two cylinders obtained by PIV measurements in a water tunnel. Hasebe *et al*. (2009) investigated the flow field between two square cylinders in tandem arrangement by measurement of surface pressure of both cylinders using split-fiber probe.

4.1 Experimental setup

Fig. 15 illustrates a PIV measurement. A laser device supplied a 532 nm laser with a light intensity of 135 mJ. The laser device had two heads which generated pulses at time intervals of 500 μs. Very fine olive oil particles of 1 μm were used for seeds. The flow field was captured by a high resolution, two-mega pixel CCD camera. Finally, the velocity vector field of the measurement range was obtained from the two captured particle images.

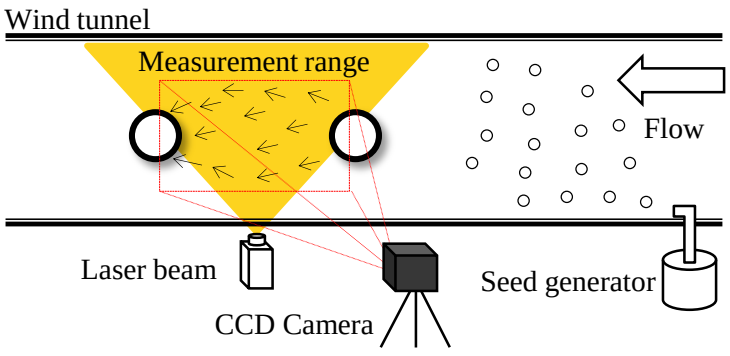

Fig. 15 PIV measurement

4.2 Change in the Scruton number for PIV measurements

During the re-setup of the cylinder models for PIV tests, the Scruton number is lowered to about 1/3, which enables better observations of the flow stream. This can be done as follows. A steel rod in the acryl model is replaced with an aluminum bar to decrease the total mass. As a result, the damping ratio decreases from 0.19% to 0.12% which corresponds to a bear stay cable. Table 2 gives the setup parameters for PIV tests.

Fig. 16 shows the amplitudes for wake galloping using the modified setup. The red line represents the allowable amplitude of the vibration. As the wind velocity increases, severe wake galloping is observed at the downstream cable. The vibrations which exceed the measurement range are observed for a spacing ratio between 3.0*D* and 5.0*D*. The amplitude of vibration decreases with increasing spacing ratio and the maximum amplitude of the vibration exceeds the limit of the guidelines up to a spacing ratio of 6.0*D*. However, spacing ratios over 7.0*D* show the vibration of acceptable amplitudes.

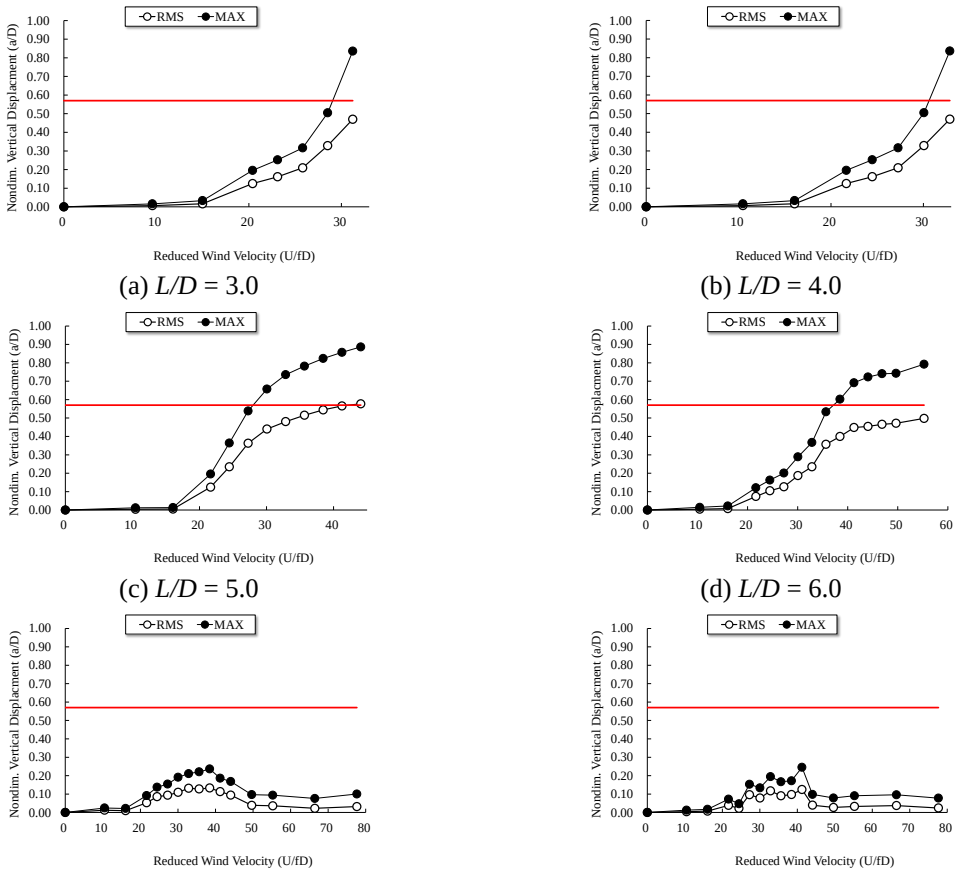

(a) *L/D* = 3.0 (b) *L/D* = 4.0

(c) *L/D* = 5.0 (d) *L/D* = 6.0

(e) *L/D* = 7.0 (f) *L/D* = 8.0

Fig. 16 RMS & Maximum value of non-dimensional vertical response of downstream cylinder with the modified setup parameters

Table 2 Change of setup parameters of cylinder model for PIV tests

Parameters	Reduced scale	Prototype	Model for normal setup	Model for PIV
Length (m)	λ_L =1/2.5	2.54	0.900	0.900
Diameter (m)	λ_L	0.250	0.100	0.100
Mass (kg/m)	λ_L^2	92.426	15.210	6.740
1st Frequency (Hz)	λ_f =3.28	0.599	1.97	2.411
Damping ratio (%)	1	0.190	0.190	0.120
Scruton number	1	2.341	2.408	0.674

4.3 Flow visualization of a single cylinder

Fig. 17 presents the shear layer for a single cylinder obtained by averaging the velocity vector behind the cylinder (Kim 2002 and Seo *et al*. 2013). The sampling rate is 15 Hz and each measuring time is 10 seconds. The shear layer can be clearly identified behind the cylinder and it becomes weakened as the distance from the cylinder increases. The length of the shear layer exceeds 50 cm which is 5 times the diameter of the cylinder.

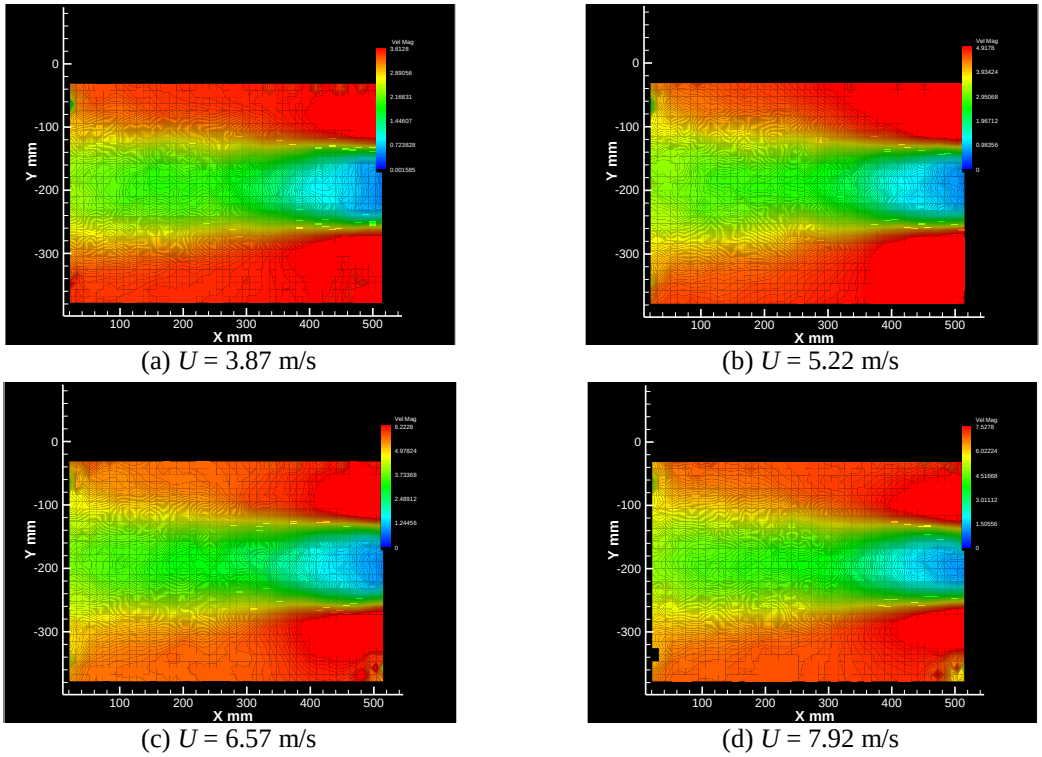

(a) U = 3.87 m/s (b) U = 5.22 m/s

(c) U = 6.57 m/s (d) U = 7.92 m/s

Fig. 17 Shear layer identified for a single cylinder

4.4 Flow visualization of two cylinders in a tandem arrangement

This experiment attempts to clarify the mechanism of wake galloping by comparing the flow field in the presence and absence of wake galloping. More specifically, the flow characteristics of the vulernable spacing ratio (L/D = 3.0) and safe spacing ratio (L/D = 7.0) for the critical wind velocity (U = 7.25 m/s) are presented in terms of a velocity vector field and by streamlines in Figs. 19 and 20, respectively.

The white circle on the right hand side of Figs. 19 and 20 represents the upstream cylinder. These figures show that significant shear layers are developed around the two cylinders. The downstream cylinder repeatedly reaches the top and bottom of the shear layer, as illustrated in Figs. 19(a) and 19(d). This phenomenon causes significant gap flows around the downstream cylinder and induces a lift force, even in the case of a small displacement.

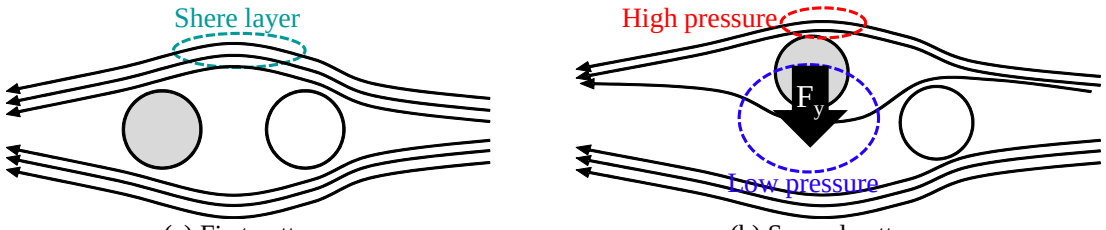

(a) First pattern (b) Second pattern

Fig. 18 Two basic flow patterns during wake galloping

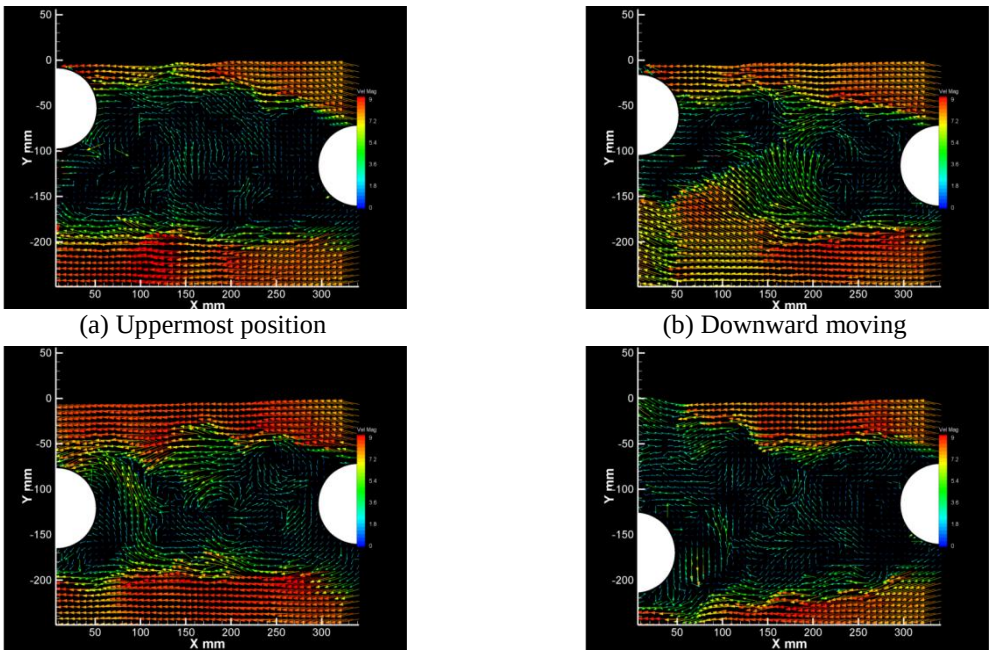

(a) Uppermost position (b) Downward moving

(c) Centerline to bottom (d) Lowermost position

Fig. 19 Velocity vector field as a function of the position of the downstream cylinder (L/D = 3.0, U = 7.25 m/s)

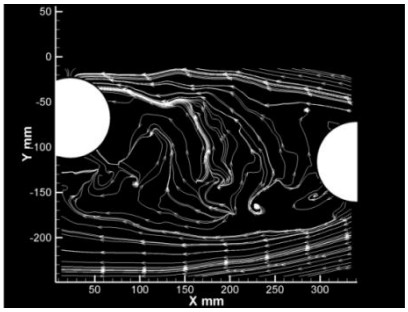

(a) Uppermost position

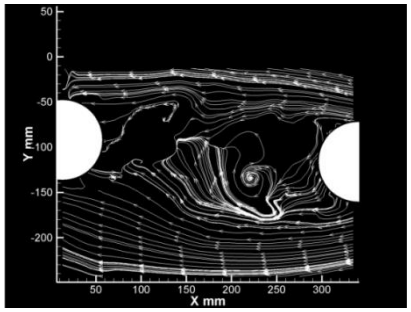

(b) Downward moving

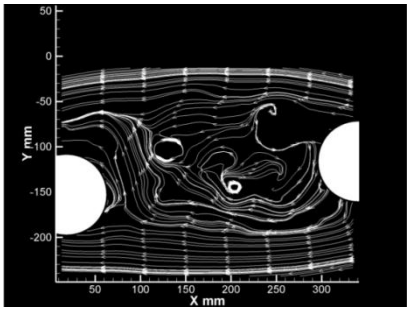

(c) Centerline to bottom

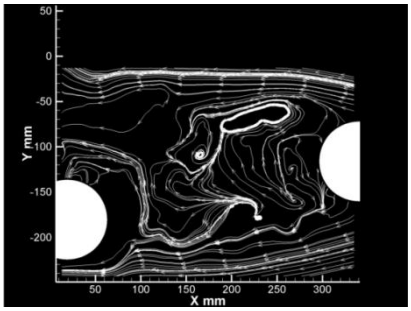

(d) Lowermost position

Fig. 20 Streamline according to the position of downstream cylinder (L/D = 3.0, U = 7.25 m/s)

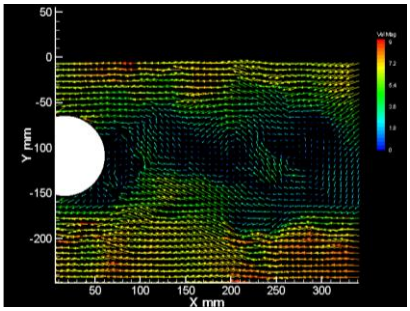

(a) At specific time 1

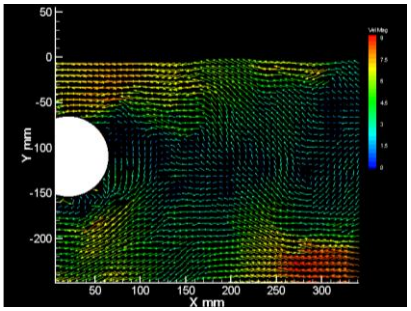

(b) At specific time 2

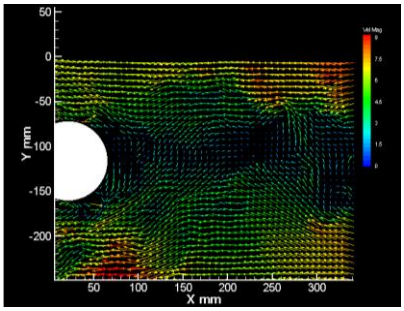

(c) At specific time 3

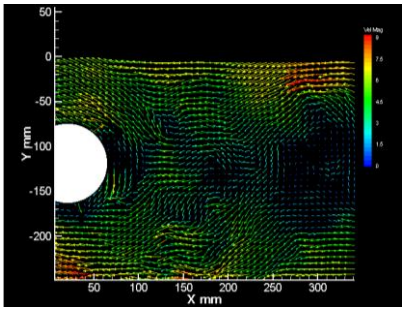

(d) At specific time 4

Fig. 21 Instantaneous velocity vector field (L/D = 7.0, U = 7.25 m/s)

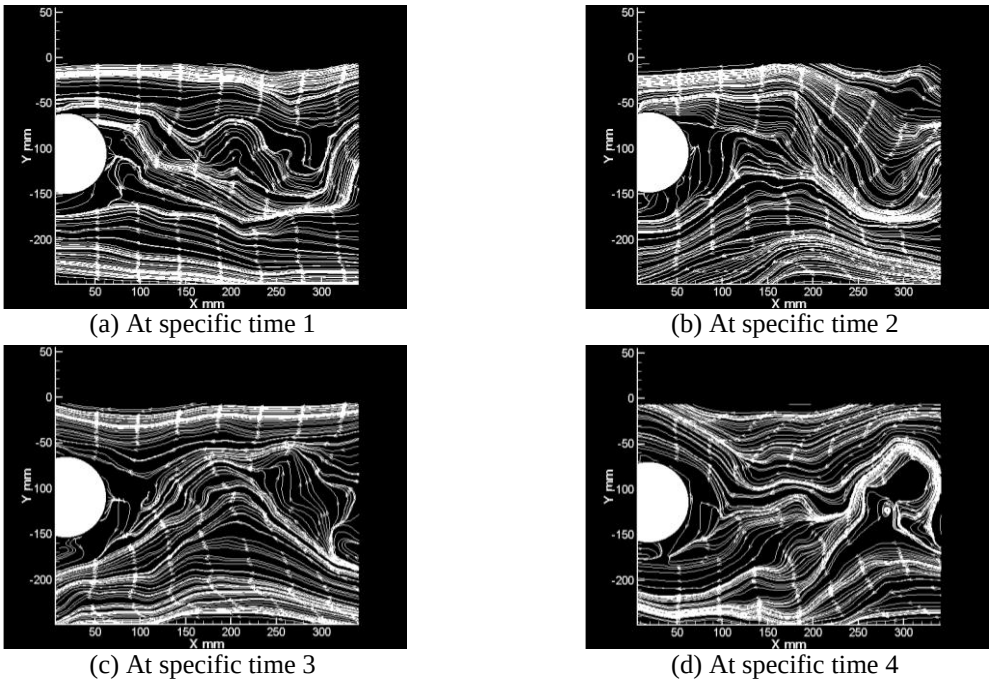

(a) At specific time 1 (b) At specific time 2

(c) At specific time 3 (d) At specific time 4

Fig. 22 Instantaneous streamline (L/D = 7.0, U = 7.25 m/s)

Figs. 21 and 22 show the case of a safe spacing ratio, in which shear layer is not identified. No regular pattern can be found in the flow around the downstream cylinder. The separation of a shear layer is also not observed in the downstream cylinder, as shown in Fig. 22.

5. Conclusions

Wake galloping between two cylinders was investigated through a sectional model wind tunnel test. The preliminary tests for parallel cylinders were in good agreement with the conventional guidelines used for estimating wake galloping vulnerability in terms of the spacing ratio between two cables. The effect of two cylinders with an unparallel disposition on wake galloping was ultimately investigated using a setup that involved two cylinders with different spacing ratios in both ends of the cylinders. The motivation for this experiment concerned an actual cable-stayed bridge in which the gap distances between two closely spaced stay cables varied from the tower to the deck anchorages. Based on the wind tunnel test results, an unparallel disposition of two cylinders was confirmed to be effective in reducing wake galloping phenomena caused by un-synchronized motion along the cylinder with varying gap spacing. The flow fields between the two cylinders were also investigated with PIV measurements. When the gap distance between the two cylinders is small, the downstream cylinder is located in the shear layer produced by the upstream cylinder. The interaction between the shear layer and the vertical motion in the downstream cylinder invokes a vertical force that causes the cylinder to return to the original position. This interaction excites the downstream cylinder in the pattern of wake galloping. However, the

interaction gradually decreases with increasing gap distance and, when the space becomes larger beyond the critical distance, the downstream cylinder becomes stable to wake galloping.

Acknowledgments

This research was supported by grants (09CCTI-A052531-06-000000) from the Ministry of Land, Transport and Maritime (MLTM) of Korean government through the Core Research Institute at Seoul National University for Core Engineering Technology Development of Super Long Span Bridge R&D Center, and also partially supported by Integrated Research Institute of Construction and Environmental Engineering at Seoul National University.

References

Assi, G.R.S., Bearman, P.W. and Meneghini, J.R. (2010), "On the wake-induced vibration of tandem circular cylinders: the vortex interaction excitation mechanism", *J. Fluid Mech.*, **661**(1), 365-401.

Błazik-Borowa, E. and Flaga, A. (1998), "Numerical analysis of interference galloping of two identical circular cylinders", *Wind Struct.*, **1**(3), 243-253.

Caetano, E. (2007), *Cable vibrations in cable-stayed bridges (Vol. 9)*, International Association for Bridge and Structural Engineering (IABSE), Zurich, Switzerland.

Cheng, S.H., Larose, G.L., Savage, M.G. and Tanaka, H. (2003), "Aerodynamic behaviour of an inclined circular cylinder", *Wind Struct.*, **6**(3), 197-208.

Cheng, S.H. and Tanaka, H. (2005), "Correlation of aerodynamic forces on an inclined circular cylinder", *Wind Struct.*, **8**(2), 135-146.

Dielen, B. and Ruscheweyh, H. (1995), "Mechanism of interference galloping of two identical circular cylinders in cross flow", *J. Wind Eng. Ind. Aerod.*, **54**, 289-300.

Hasebe, H., Watanabe, K., Watanabe, Y. and Nomura, T. (2009), "Experimental study on the flow field between two square cylinders in tandem arrangement", *Proceedings of the 7th Asia-Pacific Conference on Wind Engineering*, Taipei, Taiwan, November.

Kim, B.J., Lee, S.H. and Kim, H.K. (2012), "Mokpo bridge: new landmark in Mokpo city", *Struct. Eng. Int.*, **22**(1), 29-31.

Kim, S., Alam, M.M., Sakamoto, H. and Zhou, Y. (2009), "Flow-induced vibration of two circular cylinders in tandem arrangement. Part 2: Suppression of vibrations", *J. Wind Eng. Ind. Aerod.*, **97**(5), 312-319.

Kim, S.I. and Sakamoto, H. (2006), "Characteristics of fluctuating lift forces of a circular cylinder during generation of vortex excitation", *Wind Struct.*, **9**(2), 109-124.

Kim, S.J., Kim, H.K. and Lee, S.H. (2011), "Evaluation of wake galloping for inclined parallel cables by two-dimensional wind tunnel tests", *J. Korean Soc. Steel Constr*., **23**(6), 763-775 (in Korean)..

Kim, J.D. (2002), *Large eddy simulation of the turbulent flow around a square prism*, Ph.D. Dissertation, The University of Western Ontario, Canada.

Korea Society of Civil Engineering (KSCE) (2006), *Design guidelines for steel cable-supported bridges*, Seoul, Korea (in Korean).

Kumarasena, S., Jones, N.P., Irwin, P. and Taylor, P. (2007), *Wind-induced vibration of stay cables* (No. FHWA-RD-05-083).

Land Development Technology Research Foundation. (1989), *Review report of wind resistance of stay-cables*, Japan.

Li, Y., Wu, M., Chen, X., Wang, T. and Liao, H. (2013), "Wind-tunnel study of wake galloping of parallel cables on cable-stayed bridges and its suppression", *Wind Struct.*, **16**(3), 249-261.

Lee, S.J. and Lee, J.Y. (2008), "PIV measurements of the wake behind a rotationally oscillating circular

cylinder", *J. Fluid. Struct.*, **24**(1), 2-17.
Ozgoren, M., Pinar, E., Sahin, B. and Akilli, H. (2011), "Comparison of flow structures in the downstream region of a cylinder and sphere", *Int. J. Heat Fluid Fl.*, **32**(6), 1138-1146.
PTI Guide Specification (2001), *Recommendations for Stay Cable Design, Testing and Installation*, Post-Tensioning Institute, USA.
Seo, J.W., Kim, H.K., Park, J., Kim, K.T. and Kim G.N. (2013), "Interference effect on vortex-induced vibration in a parallel twin cable-stayed bridge", *J. Wind Eng. Ind. Aerod.*, **116**, 7-20.
SETRA. (2002),*CIP Recommendations on Cable Stays*, French International Commission on Prestressing, France.
Tokoro, S., Komatsu, H., Nakasu, M., Mizuguchi, K. and Kasuga, A. (2000), "A Study on wake-galloping employing full aeroelastic twin cable model", *J. Wind Eng. Ind. Aerod*., **88**(2-3), 247-261.

CC